

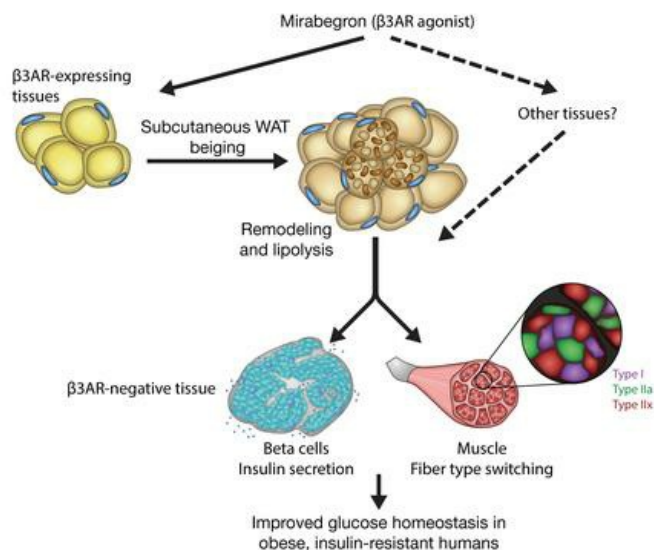
# The $\beta_3$ -adrenergic receptor agonist mirabegron improves glucose homeostasis in obese humans

Brian S. Finlin, ... , Esther E. Dupont-Versteegden, Philip A. Kern

*J Clin Invest.* 2020. <https://doi.org/10.1172/JCI134892>.

Clinical Research and Public Health In-Press Preview Metabolism

## Graphical abstract



Find the latest version:

<https://jci.me/134892/pdf>



## The $\beta$ 3-Adrenergic Receptor Agonist Mirabegron Improves Glucose Homeostasis in Obese Humans

**Brian S. Finlin<sup>1#</sup>, Hasiyet Memetimin<sup>1#</sup>, Beibei Zhu<sup>1</sup>, Amy L. Confides<sup>2</sup>, Hemendra J. Vekaria<sup>3</sup>, Riham H El Khouli<sup>4</sup>, Zachary R. Johnson<sup>1</sup>, Philip M. Westgate<sup>5</sup>, Jianzhong Chen<sup>6</sup>, Andrew J. Morris<sup>6</sup>, Patrick G. Sullivan<sup>3</sup>, Esther E. Dupont-Versteegden<sup>2</sup>, and Philip A. Kern<sup>1</sup>**

<sup>1</sup>The Department of Internal Medicine, Division of Endocrinology, and the Barnstable Brown Diabetes and Obesity Center, <sup>2</sup>Department of Physical Therapy, College of Health Sciences and Center for Muscle Biology, <sup>3</sup>Spinal Cord and Brain Injury Research Center, <sup>4</sup>Department of Radiology, <sup>5</sup>College of Public Health, <sup>6</sup>Division of Cardiovascular Medicine and Lexington Veterans Affairs Medical Center, University of Kentucky, Lexington, KY 40536.

**Address for Correspondence:** Philip A. Kern, MD  
Division of Endocrinology, CTW 521  
University of Kentucky  
900 S. Limestone St.  
Lexington, KY 40536  
Phone: 859-218-1394  
FAX: 859-257-3646  
philipkern@uky.edu

#equal contribution

The authors have declared that no conflict of interest exists.

Word Count: 4775

Figure Count: 6

Table Count: 2

Supplemental Table Count: 6

Supplemental Figure Count: 2

Keywords: brown adipose tissue, beige adipose tissue, glucose homeostasis, obesity

## **Abstract**

**BACKGROUND.** Beige adipose tissue is associated with improved glucose homeostasis in mice. Adipose tissue contains  $\beta 3$  adrenergic receptors ( $\beta 3$ -AR), and this study was intended to determine whether the treatment of obese, insulin-resistant humans with the  $\beta 3$ AR agonist mirabegron, which stimulates beige adipose formation in subcutaneous white adipose tissue (SC WAT), would induce other beneficial changes in fat and muscle, and improve metabolic homeostasis.

**METHODS.** Before and after  $\beta 3$ AR agonist treatment, oral glucose tolerance tests and euglycemic clamps were performed, and histochemistry and gene expression profiling were performed from fat and muscle biopsies. PET CT scans quantified brown adipose tissue volume and activity and we conducted in vitro studies with primary cultures of differentiated human adipocytes and muscle.

**RESULTS.** Clinical effects of mirabegron treatment included improved oral glucose tolerance ( $P < 0.01$ ), reduced hemoglobin A1c ( $P = 0.01$ ), and improved insulin sensitivity ( $P = 0.03$ ) and  $\beta$ -cell function ( $P = 0.01$ ). In SC WAT, mirabegron treatment stimulated lipolysis, reduced fibrotic gene expression and increased alternatively activated macrophages. Subjects with the most SC WAT being demonstrated the most improvement in  $\beta$ -cell function. In skeletal muscle, mirabegron reduced triglycerides, increased expression of *PGC1A* ( $P < 0.05$ ), and increased type I fibers ( $P < 0.01$ ). Conditioned media from adipocytes treated with mirabegron stimulated muscle fiber *PGC1A* expression in vitro ( $P < 0.001$ ).

**CONCLUSION.** Mirabegron treatment significantly improves glucose tolerance in obese, insulin resistant humans. Since  $\beta$ -cells and skeletal muscle do not express  $\beta 3$ -ARs, these data suggest that the beiging of SC WAT by mirabegron reduces adipose

tissue dysfunction, which enhances muscle oxidative capacity and improves  $\beta$ -cell function.

**TRIAL REGISTRATION.** Clinicaltrials.gov NCT02919176.

**FUNDING.** NIH (DK112282, P30GM127211, DK 71349, and CTSA grant UL1TR001998).

## Introduction

The  $\beta$ 3-adrenergic receptor ( $\beta$ 3-AR) has long been a therapeutic target to combat obesity and metabolic disease. Since the  $\beta$ 3-AR is present in adipose tissue, but not in most other tissues, an agonist would activate thermogenesis in adipose tissue, stimulating lipid oxidation and glucose consumption to produce heat (1, 2) without causing cardiovascular side effects. Much initial work has been performed in rodents, which maintain brown adipose tissue (BAT) throughout adulthood to defend against cold; indeed, treatment of rodents with  $\beta$ 3-AR agonists activates BAT, resulting in increased energy expenditure, weight loss, and improved glucose and lipid metabolism (3-5). In addition to stimulating white adipose tissue lipolysis, it is now recognized that  $\beta$ 3-AR activation (or cold exposure) induces the formation of brown adipocytes in SC WAT (6), which are now called beige adipocytes (7). Recent studies utilizing tissue transplantation or genetic approaches have demonstrated that beige adipose tissue is associated with improved glucose and lipid homeostasis (8-12).

BAT is highly specialized and functions to generate heat in response to activation of the sympathetic nervous system through non-shivering thermogenesis (13). The adipocytes in BAT have higher levels of mitochondria than those in WAT, and these mitochondria have high levels of uncoupling protein 1 (UCP1). Activation of the sympathetic nervous system stimulates lipolysis and UCP1 activation in BAT causing energy to be converted to heat, consuming lipids and glucose (13). BAT is present in adult humans (14-17), and is associated with improved insulin sensitivity and glucose homeostasis (recently reviewed (18)). However, BAT diminishes with both age and obesity, and there are questions about whether BAT activation is feasible

therapeutically in the older, insulin-resistant human population that would be the logical target for drug treatment (19).

Beige adipocytes are unique since they have a different developmental origin than brown adipocytes, and are highly inducible by cold exposure or  $\beta$ -AR agonism (recently reviewed in (20)). Recent studies in mice have demonstrated that beige adipocytes can activate glycolytic pathways and improve glucose metabolism independent of UCP1 (21) and that futile metabolic cycles act in addition to UCP1-mediated uncoupled respiration (21, 22). Beiging is also associated with reduced adipose tissue fibrosis and adipose dysfunction (11, 23). These findings suggest that inducing beige adipose tissue may improve metabolic homeostasis by increasing the ability of SC WAT to function as a metabolic sink for glucose and lipids (20) or by reducing white adipose tissue dysfunction that occurs with obesity (24, 25). Substantial beiging of human SC WAT has been demonstrated with cancer cachexia, burns, and conditions with high catecholamine levels (26-29), and we have demonstrated the induction of UCP1 and beige adipose markers in SC WAT in response to cold (30). However, no study in humans has demonstrated a link between beige fat and glucose or lipid metabolism.

Mirabegron is a  $\beta$ 3AR agonist that is FDA-approved for the treatment of overactive bladder at a maximal dose of 50 mg /day. In recent human studies, acute mirabegron treatment increased BAT activity and resting energy expenditure in lean humans with demonstrable baseline levels of BAT in a dose dependent manner (31-33). We treated a cohort of human research participants who were older, obese, and insulin-

resistant with mirabegron for 12 weeks and observed that chronic mirabegron treatment stimulated SC WAT beiging (30).

We now present the results of extensive metabolic phenotyping of an expanded cohort of obese, insulin resistant subjects before and after mirabegron treatment. We found that mirabegron treatment significantly improved glucose homeostasis and addressed many of the underlying mechanisms of insulin resistance, including improved insulin sensitivity and secretion and improved adipose tissue and skeletal muscle lipotoxicity and inflammation, yet had no effect on BAT in these older, obese subjects.

## Results

*Effect of mirabegron treatment on lipid and glucose homeostasis.* A flow diagram showing the subject recruitment and study design is shown in Figure 1. There was no significant change in body weight after treatment with mirabegron (Table 1). Consistent with this, mirabegron treatment did not change any measure of body composition (Table S1) or resting energy expenditure (Table S2). Mirabegron treatment did not significantly change plasma lipid levels, although there was a trend for a reduction in total cholesterol (Table 1;  $P=0.09$ ). In addition, there were no reported side effects, in particular no cardiovascular side effects such as palpitations or rapid pulse. Blood pressure and heart rate did not change with treatment (Table 1), consistent with previous studies (34).

Glucose homeostasis was assessed with an oral glucose tolerance test (OGTT) and measurement of HbA1c. Fasting blood glucose was not affected by mirabegron treatment (Table 1); however, mirabegron treatment significantly improved overall oral glucose tolerance ( $P<0.01$ ;  $n=12$ ), as shown in Figure 2A. The glucose concentration at 120 min after oral glucose ingestion was significantly lower after mirabegron treatment (Table 1;  $P<0.01$ ). A subset of subjects had impaired glucose tolerance, and 120 min glucose decreased from 165 mg/dl to 120 mg/dl after treatment. Among the 13 subjects, 9 had prediabetes according to American Diabetes Association criteria (having any of the following: fasting glucose 100-125 mg/dl; or 120 min glucose 140-199 mg/dl; or HbA1c between 5.7 and 6.4%). Following mirabegron treatment for 12 weeks, 5 of the 9 subjects were no longer prediabetic (did not have any of the criteria described above). Overall, these subjects did not have diabetes, and the mean HbA1c level of the

group was  $5.6 \pm 0.1$  at baseline (Table 1). HbA1c was significantly lower after mirabegron treatment (Table 1;  $P=0.01$ ), consistent with the overall improvement in glucose tolerance.

*Insulin sensitivity and pancreatic  $\beta$ -cell function.* To determine the underlying mechanisms for the improved glucose tolerance, we evaluated insulin sensitivity and pancreatic  $\beta$ -cell function using results obtained from both the OGTT and the euglycemic clamp. Mirabegron treatment did not significantly change baseline insulin (Table 1), nor HOMA-IR or the Matsuda index, which are measures of insulin sensitivity derived from the results of the OGTT (33). However, the results from euglycemic clamps, which are the gold standard for measuring insulin sensitivity (35), revealed that mirabegron treatment consistently and significantly increased the glucose infusion rate (GIR) by approximately 12% (Figure 2B;  $P=0.03$ ). Using glucose and insulin values from the OGTT, we calculated the insulinogenic index as an indicator of unadjusted insulin secretion. Using the insulin sensitivity from the clamp and the insulinogenic index, we then calculated insulin secretion adjusted for the insulin sensitivity, or the disposition index (36). Mirabegron treatment significantly increased both the insulinogenic index (Figure 2C;  $P=0.02$ ) and the disposition index (Figure 2D;  $P=0.01$ ), indicating improved  $\beta$ -cell function. We examined insulin levels during the OGTT (Figure S1A) and the euglycemic clamps (Figure S1B ) and did not find evidence that mirabegron changed insulin clearance rates. Finally, although weight was not significantly reduced, some subjects did weigh less after mirabegron treatment. We therefore performed an analysis to determine whether percent weight change influenced insulin sensitivity, but did not find a significant relationship ( $P=0.55$ ). Together, these

results indicate that the improved glucose tolerance was the result of both increased  $\beta$ -cell function and improved insulin sensitivity.

*Beige and brown adipose tissue.* The  $\beta$ 3-AR has a restricted tissue distribution, with expression reported in white and brown adipocytes and bladder smooth muscle cells. It is thus possible that the effects on insulin sensitivity and  $\beta$ -cell function were not direct, but the result of SC WAT beiging or brown fat induction. Indeed, both beige and brown adipose tissue activity are associated with improved glucose homeostasis and are postulated to secrete “batokines” to communicate with peripheral tissues (20). In previous studies, mirabegron was demonstrated to acutely increase BAT activity in young, lean, male subjects with detectable levels of BAT at baseline, and was more effective at higher doses (200 mg), which is 4-times the FDA approved dose (31, 32). To determine whether chronic mirabegron treatment (50 mg /day) increased BAT activity in older, insulin-resistant subjects, we performed cold-stimulated PET-CT before and after mirabegron treatment. As shown in Figure 2E, mirabegron treatment did not increase BAT volume. Notably, 8 of the subjects had no demonstrable BAT at baseline, and there was no increase of BAT in these subjects following mirabegron treatment. There was also no increase in any measure of glucose uptake by BAT (Table S3).

We previously observed that mirabegron treatment significantly induced beiging of SC WAT in six subjects (30), who were part of the 13 subjects in this report. Consistent with that study, mirabegron treatment increased the protein expression of the beige adipose markers UCP1 (2.4-fold,  $P < 0.0001$ ), transmembrane protein 26 (TMEM26) (4.2-fold,  $P < 0.001$ ), and cell death inducing DFFA like effector A (CIDEA) (2.4-fold,  $P < 0.01$ ) in SC WAT in the entire cohort ( $n=13$ ). Since mirabegron treatment

increased beige fat, we determined whether the change in adipose beiging correlated with the changes in insulin sensitivity or the disposition index. This analysis revealed that the change of UCP1 protein in SC WAT significantly correlated with the change in the disposition index, indicating a possible beneficial relationship between beige fat and pancreatic  $\beta$ -cell function (Figure 2F;  $P=0.05$ ). Although there was a relationship between the change in UCP1 protein in SC WAT and the insulinogenic index, it did not reach statistical significance ( $r=0.46$ ;  $P=0.12$ ). The change of UCP1 protein in SC WAT did not significantly correlate with the change in GIR ( $P=0.27$ ).

*Systemic inflammation and skeletal muscle lipotoxicity.* Inflammation and lipotoxicity are both implicated with the development of insulin resistance and reduced  $\beta$ -cell function in the context of obesity in humans. We measured the plasma levels of adiponectin, high molecular weight (HMW) adiponectin, tumor necrosis factor ( $TNF\alpha$ ), and monocyte chemoattractant protein 1 (MCP1). Plasma levels of  $TNF\alpha$ , MCP1, or total or HMW adiponectin did not change after mirabegron treatment (Table S4). We measured triglyceride (TG), diacylglyceride (DAG), and ceramide levels in vastus lateralis muscle biopsies to determine whether mirabegron treatment reduced lipotoxicity. Mirabegron treatment caused a slight reduction in TG levels (Figure 3A;  $P=0.04$ ), but did not reduce the lipotoxic lipids ceramide or DAG (Figure 3B and C).

We investigated mechanisms for the reduction in muscle triglyceride. Peroxisome proliferator-activated receptor gamma coactivator 1-alpha ( $PGC1\alpha$ ) is part of a transcriptional network that regulates muscle fiber-type determination and promotes fatty acid oxidation, mitochondrial biogenesis, and type I fiber formation (37, 38). *PGC1A* mRNA expression was significantly increased in muscle by mirabegron

treatment (Figure 3D;  $P < 0.05$ ). Both mitochondrial transcription factor A (*TFAM1*) and cyclooxygenase IV (*COX IV*) were increased after mirabegron treatment (Figure 3E and F;  $P < 0.01$ ), consistent with the induction of *PGC1A*. In addition to *PGC1A*, we measured the mRNA expression of perilipin 5 (*PLIN5*). *PLIN5* expression is associated with increased insulin sensitivity and this is thought to be due to its ability to promote fatty acid oxidation (39). *PLIN5* was upregulated by mirabegron treatment (Figure 3G;  $P < 0.01$ ). A possible explanation for these changes in gene expression is that mirabegron treatment changed the fiber type composition of skeletal muscle; therefore, we quantified type I, type IIa, type IIx, and type IIa /IIx fibers. As shown in Figure 3H through K, the percentage of type I fibers significantly increased ( $P < 0.01$ ), the percentage of type IIa fibers significantly decreased ( $P < 0.05$ ), and neither type IIx nor type IIa / IIx fibers changed following mirabegron treatment.

We measured the mRNA expression of the  $\beta$ 3-AR in muscle and did not detect mRNA expression by real-time reverse transcriptase polymerase chain reaction (RT PCR); as expected we were able to detect expression of the  $\beta$ 2-AR (data not shown). Activation of the  $\beta$ 2-AR causes skeletal muscle hypertrophy (40); however, we did not detect an increase in the size of the muscle fibers (data not shown), suggesting that mirabegron did not cause activation of  $\beta$ 2-ARs at the dose used in this study. Thus, these changes in skeletal muscle by mirabegron treatment are likely caused by an indirect mechanism, possibly related to SC WAT being. To test this concept in vitro, we prepared conditioned medium (CM) from adipocytes and from adipocytes treated with mirabegron for 16 hours. We then treated differentiated human myotubes with mirabegron, conditioned medium (CM) from differentiated human adipocytes, or CM

from adipocytes treated with mirabegron for 16h. CM from adipocytes did not induce *PGC1A* mRNA expression in myotubes; however, CM from adipocytes that were treated with mirabegron significantly increased *PGC1A* expression (Figure 4;  $P < 0.001$ ), suggesting that mirabegron treatment causes adipocytes to release a factor that induces *PGC1A* mRNA in muscle. As an additional control to account for any effect of mirabegron on myotubes, we harvested CM from adipocytes and then added mirabegron to it and treated myotubes with this medium. CM from adipocytes treated with mirabegron induced higher *PGC1A* expression in myotubes than media in which mirabegron was added after harvesting the CM from adipocytes. (Figure 4;  $P < 0.05$ ).

*Adipose Tissue Remodeling.* We have previously reported that phospho-hormone sensitive lipase (HSL) is increased after mirabegron treatment (30), suggesting that mirabegron stimulates cAMP-signaling in adipocytes. To determine whether mirabegron treatment stimulated lipolysis, we measured non-esterified fatty acids (NEFA) and glycerol in the conditioned medium from adipose explants from subjects before and after treatment. Glycerol was significantly higher in the medium of adipose tissue after mirabegron treatment (Figure 5A;  $P < 0.01$ ), and plasma NEFA levels were higher after mirabegron treatment (Figure 5B;  $P < 0.05$ ). Elevated plasma NEFA is thought to contribute to ectopic lipid accumulation and inhibition of insulin receptor signaling in the liver and skeletal muscle. Acute exposure of  $\beta$ -cells to NEFAs stimulates insulin secretion, but chronic exposure causes lipotoxicity and inhibits insulin secretion (41-43). As described above, ceramide and DAG levels in skeletal muscle were not elevated, despite the increase in plasma NEFA. This raises the interesting possibility that  $\beta$ 3-AR stimulation of beigeing induces compensatory mechanisms, such

as fiber-type switching to more oxidative type I muscle fibers described above, allowing for improved peripheral tissue function even in the presence of increased plasma NEFA levels.

To gain further insight into the effects of mirabegron on adipose tissue, we analyzed SC WAT gene expression before and after treatment using the Nanostring nCounter multiplex system. The panel of 160 genes consisted of adipokines, cytokines, immune cell markers, and genes involved in adipocyte function, angiogenesis, and fibrosis (Table S5). Fatty acid binding protein 4 (*FABP4*) mRNA expression was significantly induced by mirabegron treatment. *FABP4*, a lipid chaperone, is regulated by fatty acids (44) and is likely induced by mirabegron treatment in response to increased lipolysis. Collagen 6 and elastin as well as metalloproteinases and tissue inhibitors of metalloproteinases (TIMPs) were significantly changed by mirabegron treatment, and most of these were lower after treatment (Table 2), suggesting reduced extracellular matrix (ECM) remodeling. The mRNA expression of two genes encoding secreted proteins with known effects on insulin resistance were changed. Fibroblast growth factor 21 (*FGF21*), which has beneficial effects overall on metabolic homeostasis, was induced by mirabegron treatment; resistin, which is associated with insulin resistance, was suppressed by mirabegron treatment. Retinol binding protein 4 (*RBP4*) mRNA expression was elevated; *RBP4* is a secreted protein that is postulated to promote local adipose tissue inflammation; however, we did not find increased inflammatory gene expression. Also, mirabegron treatment did not affect the expression of any of the  $\beta$ ARs (Figure S2). Overall, mirabegron treatment yielded many changes in SC WAT gene expression that indicate a shift towards an improvement in adipose tissue function.

Finally, we determined whether mirabegron changed plasma levels of resistin, FGF21, adiponectin, or leptin. We did not detect significant changes in the plasma levels of any of these proteins (Table S4).

To assess adipose tissue inflammation, we measured adipose tissue macrophage polarization in response to mirabegron. CD163/CD68 macrophages were increased in SC WAT after mirabegron treatment ( $P < 0.05$ ), but CD86/CD68 macrophages were not changed (Figure 6A and B). This result indicates a shift towards M2 macrophage polarization, suggesting reduced adipose dysfunction, consistent with the results of gene expression analysis. Finally, we observed that UCP1 was often present as punctate staining in small cells between the large, unilocular adipocytes. UCP1 staining colocalized with CD163, and UCP1/CD163 positive cells significantly increase in SC WAT after mirabegron treatment (Figure 6C and D;  $P < 0.001$ ). These results suggest that UCP1 is not only present in beige adipocytes, but is also expressed in alternatively activated macrophages, which may play an important function in beige adipose tissue in humans.

*SC WAT Mitochondrial Bioenergetics.* We previously demonstrated that repeated cold exposure increased mitochondrial uncoupling in SC WAT (30). Using similar methods, we examined the bioenergetic profiles of purified mitochondria from SC WAT before and after mirabegron treatment by measuring state 3 and 4 respiration, uncoupling activity, and maximal respiration. The bioenergetic profiles before and after treatment with mirabegron are shown in Figure 7A and B. To measure UCP1-driven uncoupling, we calculated the difference between the oxygen consumption rates (OCRs) obtained during the presence of oligomycin and then free fatty acids (FFA), which are

subsequently added to stimulate uncoupling. Despite the fact that mirabegron induced UCP1 protein expression, it did not increase uncoupled respiration. However, respiration in the presence of oligomycin (State 4) was lower after mirabegron treatment (Figure 7A and B). As part of our experimental protocol, we add bovine serum albumin (BSA) after the addition of FFA to sequester the FFA, demonstrating the effects of FFA on uncoupling. The OCR after BSA addition was lower than the OCR after oligomycin addition both before (Figure 7A) and after treatment (Figure 7B), and this difference (Oligo–BSA) likely reflects stimulation of uncoupled respiration by endogenous FFAs or reactive oxygen species, both of which are sequestered by BSA. As shown in Figure 7C, Oligo–BSA was significantly lower after mirabegron treatment ( $P < 0.05$ ). The reduction in uncoupled respiration (Oligo–BSA) and increase in metabolic efficiency likely reflects a beneficial effect of mirabegron treatment on SC WAT.

*Summary and Conclusions.* Mirabegron treatment improves glucose homeostasis in humans who are obese and insulin-resistant. The underlying mechanisms involve both increased insulin sensitivity and  $\beta$ -cell function. We found that mirabegron treatment caused an increase in type I fibers in skeletal muscle and had numerous positive effects on skeletal muscle gene expression that likely arise from increased PGC1 $\alpha$  expression. These changes in muscle would be predicted to increase insulin sensitivity and fatty acid oxidation. However, we were unable to detect  $\beta$ 3-AR mRNA expression in muscle, and the  $\beta$ 3-AR is also not expressed by  $\beta$ -cells (45). Thus, the effects on both  $\beta$ -cells and muscle are likely indirect and caused by the numerous changes to SC WAT including beiging, adipose tissue remodeling, and reduced inflammation. Mirabegron did not induce BAT and we found no evidence for increased uncoupled respiration or

lipid oxidation even though mirabegron treatment induced UCP1 protein expression in SC WAT. Furthermore, the beneficial physiological effects of mirabegron treatment on glucose metabolism, insulin sensitivity, and  $\beta$ -cell function occurred paradoxically in the presence of increased plasma NEFA. The increased NEFA did not result in muscle lipotoxicity, which may be due to an increase in type I fibers, suggesting that protective mechanisms are induced by mirabegron treatment. This human study supports the previously suggested concept that adipose beiging has beneficial effects on glucose metabolism, which can be UCP1-independent (21).

## Discussion

Considerable evidence points to BAT and beige adipose tissue as both a metabolic sink for glucose and lipids and as a source of “batokines” that affect peripheral tissues (20).  $\beta$ 3-AR activation is currently the best known pharmacological approach for stimulating brown and beige fat, and the  $\beta$ 3-AR agonist mirabegron has recently been demonstrated to be effective at activating BAT and inducing beige adipose in humans (30-32). The current study differs from previous ones in several important ways. In this study, we targeted an at-risk population: subjects with metabolic syndrome or prediabetes rather than lean, healthy subjects. In addition, the standard FDA approved dose of mirabegron was used for 12 weeks, which is very well tolerated, whereas previous studies used this  $\beta$ 3 agonist only acutely and sometimes in doses that had cardiovascular side effects. Finally, this study was focused on both SC WAT beiging as well as BAT, along with a mechanistic examination of adipose and muscle.

The main findings of this study are that mirabegron treatment improved glucose metabolism in the absence of weight loss, and this improvement in glucose metabolism was clinically significant. Indeed, a recent study suggests that in a population of non-diabetic subjects, changes in glucose tolerance or A1C, as observed in our study, would be expected with a weight loss of more than 16% (46). Finally, our observations that mirabegron treatment had beneficial effects (increased both insulin sensitivity and  $\beta$ -cell function) on cell types that do not express the  $\beta$ 3-AR are novel, suggesting that SC WAT beiging impacts the function of peripheral tissues. Indeed, we identified a significant correlation between the change in SC WAT UCP1 and the change in the disposition index, but not with the change in insulin sensitivity. Furthermore, we were

not able to identify plasma adipokines that changed in response to mirabegron treatment. This suggests that mirabegron treatment may have had only a modest effect on adipose tissue, or caused other tissues that express the  $\beta$ 3AR to influence peripheral tissues involved in glucose homeostasis. Indeed, a recent study in lean humans demonstrated that mirabegron influences bile acid metabolism (32).

The effects of mirabegron on metabolism have recently been studied in mice, and there are notable differences between those studies (5, 47) and this study in humans. For instance, mirabegron treatment of ApoE<sup>-/-</sup> mice increased total and LDL cholesterol and promoted atherosclerosis (47), but our current study in humans found a trend for decreased cholesterol and no evidence for an increase in LDL. In another study in mice, mirabegron improved insulin sensitivity and glucose tolerance, but also induced weight loss and significantly increased BAT activity (5). In this human study, mirabegron treatment clearly affected the function of peripheral tissues involved in glucose homeostasis, but there was no weight loss and BAT activation was not a factor; the presence of BAT in mice but not obese humans likely contributes to the different responses. Other studies have demonstrated that both cold and mirabegron are capable of recruiting BAT in humans (31, 32, 48-51). However, the research participants in those studies were usually lean and younger than this study and some were pre-selected as having demonstrable BAT. Older, obese humans often have little or no demonstrable BAT (16, 52). One study did demonstrate detectable BAT in men with obesity but used a prolonged cold exposure protocol (53). The inability of mirabegron treatment to recruit BAT in this study is likely because of the low levels of BAT at baseline due to the increased age and obesity of this cohort.

Although adults with obesity have little BAT, there is considerable WAT, and both cold and mirabegron stimulate SC WAT browning, with increases in UCP1, CIDEA and TMEM26 (Finlin 2018). In spite of a clear mirabegron-induced increase in UCP1 protein expression in SC WAT, we did not detect an increase in uncoupled respiration in purified mitochondria from WAT. In a previous study using the same methods, cold exposure of lean subjects increased uncoupled respiration in mitochondria isolated from SC WAT with a similar level of induction of UCP1 (30). The reasons for the failure of mirabegron to induce uncoupling activity are unclear, but could be that mirabegron induced CIDEA, an inhibitor of UCP1 activity (54). Mirabegron may have affected reactive oxygen species (ROS) levels, which are necessary to activate UCP1 (55).

Although there was no increase in uncoupled respiration with mirabegron, the increase in lipolysis observed in this study and the increase in HSL phosphorylation on a serine residue that is a protein kinase A site (serine 660) reported previously (30) suggest that mirabegron stimulated cAMP signaling in SC WAT. Furthermore mirabegron treatment caused numerous changes in gene expression, most of which are predicted to reduce adipose tissue dysfunction. We attempted to identify changes in the plasma levels of adipokines and in proteins whose adipose gene expression was altered by mirabegron to gain mechanistic understanding into the improvement of glucose metabolism. For instance, FGF21 has many favorable metabolic effects and was upregulated in SC WAT after mirabegron treatment (56). Resistin was initially discovered as a factor secreted by adipocytes that causes insulin resistance in mice (57). Studies of resistin in humans initially yielded conflicting results; however, two large studies identified resistin as a risk factor for the development of diabetes (58, 59).

We were not able to identify changes in the plasma levels of FGF21, resistin, adiponectin, leptin, or adipisin. Overall, our findings suggest that mirabegron treatment affected many different pathways that impact adipose tissue function, and it will be important to identify mechanisms linking changes in SC WAT to improved glucose homeostasis in future studies.

One of the most interesting findings from this study was the change in skeletal muscle fiber types. The switch in muscle fiber type induced by mirabegron treatment is rather remarkable since muscle fiber type is relatively resistant to a transition from type II to type I even with significant interventions such as exercise and weight loss (60, 61). The  $\beta$ 2-AR is expressed in muscle and administration of  $\beta$ 2-AR agonists causes hypertrophy as well as a shift from type I to type II fibers (62, 63). We did not detect an increase in fiber size or type I to type II switching, suggesting that mirabegron did not activate  $\beta$ 2-ARs, consistent with the lack of cardiovascular side effects. Mirabegron increased *PGC1A* mRNA levels as well as genes regulated by *PGC1 $\alpha$* . *PGC1 $\alpha$*  promotes type I fiber induction in mice (38), and the increase in *PGC1 $\alpha$*  after mirabegron treatment is thus likely important for a number of the changes we observed including the observation that lipotoxicity was not increased despite increased plasma NEFA and insulin sensitivity was increased. It will therefore be important to identify the mechanism for *PGC1 $\alpha$*  induction by mirabegron treatment and to consider that beige adipose may be the source of the factor.

$\beta$ -cell function was increased by mirabegron treatment. A recent study in mice demonstrated an acute effect of  $\beta$ 3-AR agonism on insulin secretion and this effect was entirely dependent upon adipose tissue lipolysis since it was completely blocked in mice

with adipose tissue triglyceride lipase (ATGL) deficiency (45). This observation suggests that the  $\beta$ 3-AR is not expressed on pancreatic  $\beta$ -cells in rodents and illustrates communication between adipose tissue and  $\beta$ -cells. In addition to NEFAs, adiponectin, leptin, and adipsin are proteins secreted from adipose tissue that have an impact on  $\beta$ -cells (64-66). The results of our study indicate that the change in the disposition index, a measure of  $\beta$ -cell function, correlated with both the change in SC WAT UCP1 expression and the change in plasma NEFA, suggesting a relationship between the effect of mirabegron on SC WAT and  $\beta$ -cell function. It is possible that this effect is mediated directly by increased NEFA. It will be important to determine whether this effect persists under longer term mirabegron treatment. Although NEFAs stimulate  $\beta$ -cell insulin secretion acutely, the compensatory mechanisms of  $\beta$ -cells during chronic exposure to increased NEFAs are detrimental to insulin secretion (41-43). Another possibility is that stimulation of beige adipose results in the release of additional factors that protect  $\beta$ -cell function.

A leading hypothesis for the development of adipose dysfunction in obesity is adipocyte expansion against a rigid ECM, leading to adipocyte necrosis and macrophage recruitment (24, 25, 67). Mirabegron treatment resulted in reduced mRNA expression of collagen VI and a number of genes involved in adipose tissue remodeling. Although mirabegron treatment induced lipolysis, we did not observe any change in adipocyte size (not shown). This suggests that the changes in ECM gene expression may be due to the induction of beiging, which is linked to reduced fibrosis and a less rigid ECM (11, 23). In addition to the changes in ECM genes, the number of alternatively activated macrophages (CD163/68) increased in SC WAT after mirabegron

treatment, suggesting an environment that is less inflammatory, and more reparative. Macrophages have been reported to be recruited into adipose tissue in response to increased lipolysis to buffer free fatty acids (68). We observed that the CD163/68 macrophages recruited into SC WAT express UCP1. Although uncoupling activity in the adipose tissue did not increase overall, it is possible that UCP1 is active in these macrophages as a mechanism of oxidizing lipids. UCP1 is also expressed in CD206 positive macrophages, which increased after mirabegron treatment but did not reach statistical significance (not shown;  $P=0.12$ ). The identification of UCP1 in adipose tissue macrophages (Figure 6C) explains in part the punctate nature of UCP1 staining that we observe in human WAT.

*Limitations of the study.* This study was designed to be a proof of concept study since  $\beta$ 3AR agonists have not been studied in obese human research participants, and we sought to comprehensively characterize the response to mirabegron using both basic science and clinical techniques. This study was not placebo-controlled, and the majority of the subjects were female. A randomized, blinded placebo controlled study with a larger number of participants and males will be necessary to determine whether there are gender differences and to identify small changes that may have been missed in this study. For instance, our data indicate that mirabegron at the FDA-approved dose of 50 mg per day is specific for  $\beta$ 3ARs, which is based on a lack of cardiovascular side effects. With the sample size of this study, we cannot completely rule out  $\beta$ 2AR agonism, which could, for instance, affect  $\beta$ -cell function directly or indirectly via other cells in the islet. A placebo control group will also be necessary to rule out a placebo effect in some of the small changes identified in this study, such as the small but

consistent increase in GIR. Despite these limitations, this study forms a strong basis for future studies on mirabegron as described below.

*Conclusions, perspectives, and future goals.*  $\beta$ 3-AR agonists were initially developed as anti-obesity agents. Although  $\beta$ 3-AR agonists induce weight loss in rodents, we did not observe weight loss in this study. This could be due to the relatively low levels of BAT in humans, the mirabegron dose used, or the fact that humans will compensate for increased energy expenditure with increased food intake. Alternatively, it is possible that the 50 mg/day dose is too low to induce beiging and UCP1 activation to a level that would increase energy expenditure and weight loss. However, even without weight loss or BAT activation, this relatively low dose was sufficient to improve insulin sensitivity and  $\beta$ -cell function, despite the fact the NEFA levels increased. Higher doses of mirabegron would likely induce stronger beiging and increased lipid oxidation, which may reduce NEFA; however, unwanted cardiovascular side effects may be limiting (31, 32). It will be important to determine whether long-term mirabegron treatment at the dose used in this study would maintain improved  $\beta$ -cell function and delay the onset of diabetes in pre diabetic subjects. Finally, it would be important to know whether mirabegron improves glucose homeostasis in persons with type 2 diabetes.

## Methods

*Study design and human subjects.* This study was intended to examine the metabolic effects of mirabegron in human research participants with obesity and insulin-resistance at the dose approved by the FDA for overactive bladder. Hence, we recruited 13 sedentary subjects with a BMI >27, 35-65 years old, who had either prediabetes, on the basis of HbA1c and a standard 75 g oral glucose tolerance test (OGTT), or who had normal glucose tolerance (NGT) but with >3 features of metabolic syndrome (MetS). Nine of the thirteen subjects met at least one criteria for prediabetes at baseline: impaired fasting glucose (100-125 mg/dl), impaired glucose tolerance (120 min glucose 140-199 mg/dl), or HbA1c 5.7-6.4%. In addition to the OGTT, baseline studies included body composition by DEXA scan and resting metabolic rate (RMR) with a metabolic cart, performed fasting, early in the morning in a quiet room with temperature controlled at 22°C. Other baseline studies include a euglycemic clamp, SC WAT and muscle (vastus lateralis) biopsies, and PET-CT scans under cold stimulation to quantify BAT. Subjects were recruited from the Lexington, KY area throughout the year, and all subjects had normal thyroid function and were not taking any medications that would interfere with the study, such as  $\beta$ -blockers, steroids, or insulin sensitizers and no subjects had any chronic inflammatory conditions. Subjects were asked to continue their usual diet and level of activity. After completing the baseline studies (OGTT, clamp, fat and muscle biopsies and PET-CT), the research participants were treated with mirabegron (50 mg / day) for 12 weeks, after which the initial studies were repeated. The Clinicaltrials.gov identifier is NCT02919176.

*Biopsies.* Adipose tissue was obtained through an incisional biopsy from the abdomen, as described (69). From the abdomen, approximately 4 g of tissue was removed, most of which was used for the preparation of mitochondria for mitochondrial bioenergetics (30). The remainder was either frozen at -80 C or used for immunohistochemistry. A muscle biopsy from the vastus lateralis was also obtained using a Bergstrom needle as described previously (70). Briefly, approximately 100 mg of each biopsy was mounted with fibers perpendicular to a cork using tragacanth gum; this was snap frozen in liquid nitrogen-cooled isopentane and then stored at -80°C until sectioning.

*Euglycemic clamp.* Peripheral insulin sensitivity was measured using a euglycemic clamp, as described previously (71). Subjects arrived fasting, IVs were inserted, and euglycemia was maintained through the variable infusion of 20% glucose and frequent blood glucose measurement during an insulin infusion of 1.0 mU/kg/min. A steady state was generally attained at 2-hours, and the glucose infusion rate was determined during the final 30 min.

*Assessment of BAT.* Cold-stimulated PET-CT for measurement of BAT was performed as described previously (31, 72). After an overnight fast, subjects were brought to the PET-CT suite 120 min prior to the scan and outfitted with a cooling vest that circulated water at 14°C. At 60 min prior to scan, 440 MBq of <sup>18</sup>F-FDG was injected IV. Images were acquired using a Discovery LS multidetector helical PET-CT scanner (GE Medical Systems). PET data were acquired from the eyes to thighs and both PET and CT images were reconstructed as axial sections at 4.25-mm spacing and then reformatted by the viewer software. BAT mass and activity were quantified using the PET-CT Viewer shareware, and BAT in each axial slice was classified on a pixel-by-pixel basis

when CT was in the range -250 to -10 Hounsfield Units and when maximal standard uptake value (SUV<sub>max</sub>) ≥ 2.0 in the cervical, supraclavicular, and anterior thoracic depots from C3 to T7. Areas of <sup>18</sup>F-FDG uptake on PET colocalizing with regions of fat identified on CT were quantified by their SUV<sub>avg</sub>, and detectable BAT volume was calculated as the sum of pixels meeting this classification criteria multiplied by the pixel volume (64.8 mm<sup>3</sup>).

*Immunohistochemistry on adipose tissue and muscle.* Immunohistochemistry (IHC) and quantification of UCP1, TMEM26, and CIDEA in SC WAT was performed as described (30). We performed IHC for macrophages (CD163/CD68, CD206/CD68, or CD86/CD68) on 5 μm formalin-fixed, paraffin-embedded SC WAT sections. Tissue was deparaffinized and then blocked with hydrogen peroxide, rinsed, and blocked first with Streptavidin/Biotin blocking kit (#SP-2002, Vector) followed with 2.5% horse serum. M1 macrophages were identified by costaining with rabbit anti-CD86 (#ab53004, Abcam) and mouse anti-CD68 (#ab955, Abcam) antibodies; M2 macrophages were identified rabbit anti-CD163 (#ab182422, Abcam) and CD68 antibodies. The primary antibodies were incubated individually overnight in 1% horse serum. We determined the number of CD163 macrophages that costained with UCP1 using mouse anti-CD163 (#HM2157, Hycult Biotech) and rabbit anti-UCP1 (custom antibody # J2648, ECM biosciences). Amplification was performed with either goat anti-mouse IgG biotin (#115-065-205, Jackson ImmunoResearch) or donkey anti-rabbit IgG biotin (#711-065-152, Jackson ImmunoResearch) then Streptavidin-HRP (#S911, Thermo Fisher Scientific) followed by washing and incubation with AlexaFluor tyramide reagent (Thermo Fisher Scientific). Sections were mounted and nuclei stained using Vectashield Antifade mounting media

with 4,6-diaminidino-2-phenylindole DAPI (#H-1800, Vector Laboratories).

Macrophages were counted when cells were triple stained with CD68, CD86 or CD163, and DAPI. UCP1 positive CD163 positive cells were triple stained with CD163, UCP1, and DAPI. Macrophages were counted within fields of adipocytes and not in connective tissue. All data are normalized to adipocyte number. Images were captured with an upright Zeiss fluorescent microscope.

We performed IHC on muscle biopsies obtained from the vastus lateralis as described previously (Murach et al. 2017). Briefly, frozen muscle sections were cut at 8  $\mu$ m, air-dried, and stored at  $-20^{\circ}\text{C}$ . Sections were incubated overnight with isotype specific anti-mouse antibodies for MyHC I IgG2B (BA.D5), MyHC IIa IgG1 (SC.71) and MyHC IIx (6H1) obtained from the Developmental Studies Hybridoma Bank. Sections were then incubated with the following secondary antibodies: goat anti-mouse IgG2b Alexa fluor 647; anti-mouse IgG1 Alexa fluor 488; and anti-mouse IgM Alexa fluor 555 (Invitrogen), mounted using Vectashield anti-fade mounting media, and post fixed in methanol. Five to seven images were captured at 20x magnification using an upright fluorescence microscope (AxioImager M1; Zeiss, Oberkochen, Germany). Fiber type distribution was quantified manually in a blinded manner.

mRNA quantification. Muscle and adipose mRNA was isolated using trizol extraction and purification with RNeasy Lipid Tissue Mini kits (Qiagen, Valencia, CA). The quantity and quality was RNA determined using an Agilent 2100 Bioanalyser (Palo Alto, CA). Multiplex analysis of SC WAT gene expression was performed using the Nanostring nCounter system and a custom code set (Nanostring, Seattle, WA). The data were normalized to the geometric mean of six housekeeping genes; the genes and

accession numbers of the custom code set are in Table S5. Muscle gene expression was analyzed by real-time RT PCR as described (69), and the data were normalized to the geometric mean of six housekeeping genes (*ACTB*, *PPIA*, *PPIB*, *TBP*, *TUBB*, *UBC9*). The primer sequences are shown in Table S6.

*Quantification of lipids in muscle biopsies.* Approximately 10 mg of the vastus lateralis biopsy was weighed and then extracted with acidified organic solvents. DG and ceramides were quantified as described (73). TG were quantified in the extract using colorimetric triglyceride assays (T7532, Point Scientific, Canton, MI) as follows. 10  $\mu$ l of the lipid extract was dried for 5 min. 10  $\mu$ l 0.1% SDS in 0.9% NaCl was added and then incubated for 10 min at 37°C. One ml pre warmed triglyceride reagent was added and the reaction was incubated at 37°C for 5 min. The absorbance ( $A_{500}$ ) was measured with a spectrophotometer (Biorad) within 30 min. Lipid levels were normalized to tissue weight.

*Myotube treatment with adipocyte CM.* Adult derived human adipocyte stem cells (ADHASC) were cultured and differentiated as described previously (74). In brief, preadipocytes were incubated for 48 hours after reaching confluence and induced to differentiate into adipocytes with adipocyte differentiation medium (50% DMEM: 50% Ham's F-10), 3% FBS (Invitrogen, Carlsbad, CA), 15 mM HEPES pH 7.4, 33  $\mu$ M Biotin (Sigma, St. Louis MO), 17  $\mu$ M pantothenate (Sigma), 1  $\mu$ M dexamethasone (Sigma), 0.25 mM IBMX (Sigma),  $1 \times 10^{-7}$  M Insulin (Novo Nordisk Bagsværd, Denmark) and 1  $\mu$ M rosiglitazone (SmithKline Beecham, Welwyn Garden City, United Kingdom)) for 3 days. The cells were then incubated with adipocyte differentiation medium without IBMX and rosiglitazone with medium changes every 3 days until 80–90% of the cells

had lipid droplets (7 to 10 days). Adipocyte CM was prepared by incubating differentiated ADAHASC with DMEM with 2% FBS for 24 h and then in DMEM with 2%FBS and 0.1% DMSO (vehicle control) or 100nM mirabegron (Cayman Chemical, Ann Arbor, MI) for 16h. We also isolated CM and added mirabegron to this medium (100 nM). Adipocyte CM was filtered with a 0.2  $\mu$ m filter and frozen at -80°C for later use. Primary myoblasts from human skeletal muscle biopsies of normal subjects were provided by Dr. Charlotte Peterson (University of Kentucky). The myoblasts were differentiated in DMEM with 2% FBS for 10 days. Fully differentiated myotubes were treated with 25 nM mirabegron or 25% adipocyte conditioned medium for 16 h, and total RNA was prepared for mRNA expression analysis using real-time RT PCR.

*NEFA and glycerol measurements in plasma and adipose explant secretions.* Adipose explant secretions were prepared by incubating 0.5g of the SC WAT biopsy in 2 ml Ringer's solution supplemented with 1% lipid free BSA at 37°C for 1 h. Glycerol in the explant secretion was then measured with a high sensitivity free glycerol fluorometric assay kit (MAK270, Sigma, and St. Louis, MO). Glycerol in plasma was measured with free glycerol reagent (F6428, Sigma). NEFA in plasma or adipose explant secretions was measured with HR Series NEFA-HR(2) Color Reagents (999-34691, 995-34791, 991-34891, 993-35191, FUJIFILM Wako Diagnostics, Mountain View, CA)

*Mitochondrial Bioenergetics.* Bioenergetics of mitochondria purified from the SC WAT biopsies were determined using an Oxytherm System as previously described (30).

*Statistical analysis of data.* Paired student's t-tests or a Wilcoxon matched-pairs signed rank test were performed to compare the results before and after mirabegron treatment. Oral glucose tolerance was assessed by repeated measures two-way ANOVA with a

Siadk's multiple comparison test. Spearman correlations were used to assess associations between beiging, plasma NEFA, and  $\beta$ -cell function. Multiple comparisons were analyzed by one-way ANOVA and a Tukey multiple comparison test. Data were analyzed using Graphpad Prism version 8.0 (San Diego, CA). The method of analysis for each experiment is indicated in the figure legend. All tests were two-sided and statistical significance was set at  $P \leq 0.05$ .

*Study Approval.* All subjects gave informed consent, and the protocols were approved by the Institutional Review Board at the University of Kentucky.

**Author Contributions.**

PK, EDV, PS, CA, AM, and BF designed the experiments, analyzed data, and wrote the manuscript. BZ, HM, AC, IK, BH, KJ, ZJ, JC, and HV performed the experiments. PW analyzed data.

**Acknowledgements.**

We wish to thank the staff of the University of Kentucky Clinical Research Unit for the assistance with this study and Dorothy Ross for coordinating the recruitment of the participants. We acknowledge Rachel Davidowitz for help with the graphical abstract. This study was funded by DK112282, P30GM127211, DK 71349, and by CTSA grant UL1TR001998.

## References

1. Arch JR. Challenges in beta(3)-Adrenoceptor Agonist Drug Development. *Ther Adv Endocrinol Metab.* 2011;2(2):59-64.
2. Arch JR. beta(3)-Adrenoceptor agonists: potential, pitfalls and progress. *European journal of pharmacology.* 2002;440(2-3):99-107.
3. Arch JR, Ainsworth AT, Ellis RD, Piercy V, Thody VE, Thurlby PL, et al. Treatment of obesity with thermogenic beta-adrenoceptor agonists: studies on BRL 26830A in rodents. *Int J Obes.* 1984;8 Suppl 1:1-11.
4. Arch JR, and Ainsworth AT. Thermogenic and antiobesity activity of a novel beta-adrenoceptor agonist (BRL 26830A) in mice and rats. *Am J Clin Nutr.* 1983;38(4):549-58.
5. Hao L, Scott S, Abbasi M, Zu Y, Khan MSH, Yang Y, et al. Beneficial Metabolic Effects of Mirabegron In Vitro and in High-Fat Diet-Induced Obese Mice. *J Pharmacol Exp Ther.* 2019;369(3):419-27.
6. Frontini A, and Cinti S. Distribution and development of brown adipocytes in the murine and human adipose organ. *Cell Metab.* 2010;11(4):253-6.
7. Wu J, Bostrom P, Sparks LM, Ye L, Choi JH, Giang AH, et al. Beige adipocytes are a distinct type of thermogenic fat cell in mouse and human. *Cell.* 2012;150(2):366-76.
8. Seale P, Conroe HM, Estall J, Kajimura S, Frontini A, Ishibashi J, et al. Prdm16 determines the thermogenic program of subcutaneous white adipose tissue in mice. *The Journal of clinical investigation.* 2011;121(1):96-105.
9. Cohen P, Levy JD, Zhang Y, Frontini A, Kolodin DP, Svensson KJ, et al. Ablation of PRDM16 and beige adipose causes metabolic dysfunction and a subcutaneous to visceral fat switch. *Cell.* 2014;156(1-2):304-16.
10. Min SY, Kady J, Nam M, Rojas-Rodriguez R, Berkenwald A, Kim JH, et al. Human 'brite/beige' adipocytes develop from capillary networks, and their implantation improves metabolic homeostasis in mice. *Nature medicine.* 2016;22(3):312-8.
11. Hasegawa Y, Ikeda K, Chen Y, Alba DL, Stifler D, Shinoda K, et al. Repression of Adipose Tissue Fibrosis through a PRDM16-GTF2IRD1 Complex Improves Systemic Glucose Homeostasis. *Cell Metab.* 2018;27(1):180-94 e6.
12. Chen Y, Ikeda K, Yoneshiro T, Scaramozza A, Tajima K, Wang Q, et al. Thermal stress induces glycolytic beige fat formation via a myogenic state. *Nature.* 2019;565(7738):180-5.
13. Cannon B, and Nedergaard J. Brown adipose tissue: function and physiological significance. *Physiological reviews.* 2004;84(1):277-359.
14. van Marken Lichtenbelt WD, Vanhommerig JW, Smulders NM, Drossaerts JM, Kemerink GJ, Bouvy ND, et al. Cold-activated brown adipose tissue in healthy men. *NEnglJMed.* 2009;360(15):1500-8.
15. Virtanen KA, Lidell ME, Orava J, Heglind M, Westergren R, Niemi T, et al. Functional brown adipose tissue in healthy adults. *N Engl J Med.* 2009;360(15):1518-25.
16. Saito M, Okamatsu-Ogura Y, Matsushita M, Watanabe K, Yoneshiro T, Nio-Kobayashi J, et al. High incidence of metabolically active brown adipose tissue in healthy adult humans: effects of cold exposure and adiposity. *Diabetes.* 2009;58(7):1526-31.
17. Cypess AM, Lehman S, Williams G, Tal I, Rodman D, Goldfine AB, et al. Identification and importance of brown adipose tissue in adult humans. *NEnglJMed.* 2009;360(15):1509-17.
18. Klepac K, Georgiadi A, Tschop M, and Herzig S. The role of brown and beige adipose tissue in glycaemic control. *Mol Aspects Med.* 2019.
19. Porter C, Chondronikola M, and Sidossis LS. The Therapeutic Potential of Brown Adipocytes in Humans. *Frontiers in endocrinology.* 2015;6:156.

20. Kajimura S, Spiegelman BM, and Seale P. Brown and Beige Fat: Physiological Roles beyond Heat Generation. *Cell Metab.* 2015;22(4):546-59.
21. Ikeda K, Kang Q, Yoneshiro T, Camporez JP, Maki H, Homma M, et al. UCP1-independent signaling involving SERCA2b-mediated calcium cycling regulates beige fat thermogenesis and systemic glucose homeostasis. *Nature medicine.* 2017;23(12):1454-65.
22. Kazak L, Chouchani ET, Jedrychowski MP, Erickson BK, Shinoda K, Cohen P, et al. A creatine-driven substrate cycle enhances energy expenditure and thermogenesis in beige fat. *Cell.* 2015;163(3):643-55.
23. Wang W, Ishibashi J, Trefely S, Shao M, Cowan AJ, Sakers A, et al. A PRDM16-Driven Metabolic Signal from Adipocytes Regulates Precursor Cell Fate. *Cell Metab.* 2019;30(1):174-89 e5.
24. Crewe C, An YA, and Scherer PE. The ominous triad of adipose tissue dysfunction: inflammation, fibrosis, and impaired angiogenesis. *The Journal of clinical investigation.* 2017;127(1):74-82.
25. Sun K, Kusminski CM, and Scherer PE. Adipose tissue remodeling and obesity. *JClinInvest.* 2011;121(6):2094-101.
26. Sidossis LS, Porter C, Saraf MK, Borsheim E, Radhakrishnan RS, Chao T, et al. Browning of Subcutaneous White Adipose Tissue in Humans after Severe Adrenergic Stress. *Cell Metab.* 2015;22(2):219-27.
27. Petruzzelli M, Schweiger M, Schreiber R, Campos-Olivas R, Tsoli M, Allen J, et al. A switch from white to brown fat increases energy expenditure in cancer-associated cachexia. *Cell Metab.* 2014;20(3):433-47.
28. Frontini A, Vitali A, Perugini J, Murano I, Romiti C, Ricquier D, et al. White-to-brown transdifferentiation of omental adipocytes in patients affected by pheochromocytoma. *Biochimica et biophysica acta.* 2013;1831(5):950-9.
29. Kir S, White JP, Kleiner S, Kazak L, Cohen P, Baracos VE, et al. Tumour-derived PTH-related protein triggers adipose tissue browning and cancer cachexia. *Nature.* 2014;513(7516):100-4.
30. Finlin BS, Memetimin H, Confides AL, Kasza I, Zhu B, Vekaria HJ, et al. Human adipose beiging in response to cold and mirabegron. *JCI Insight.* 2018;3(15).
31. Cypess AM, Weiner LS, Roberts-Toler C, Elia EF, Kessler SH, Kahn PA, et al. Activation of Human Brown Adipose Tissue by a beta3-Adrenergic Receptor Agonist. *Cell Metab.* 2015;21(1):33-8.
32. Baskin AS, Linderman JD, Brychta RJ, McGehee S, Anflick-Chames E, Cero C, et al. Regulation of Human Adipose Tissue Activation, Gallbladder Size, and Bile Acid Metabolism by a beta3-Adrenergic Receptor Agonist. *Diabetes.* 2018;67(10):2113-25.
33. Loh RKC, Formosa MF, La Gerche A, Reutens AT, Kingwell BA, and Carey AL. Acute metabolic and cardiovascular effects of mirabegron in healthy individuals. *Diabetes Obes Metab.* 2019;21(2):276-84.
34. Nitti VW, Chapple CR, Walters C, Blauwet MB, Herschorn S, Milsom I, et al. Safety and tolerability of the beta3 -adrenoceptor agonist mirabegron, for the treatment of overactive bladder: results of a prospective pooled analysis of three 12-week randomised Phase III trials and of a 1-year randomised Phase III trial. *International journal of clinical practice.* 2014;68(8):972-85.
35. Pisprasert V, Ingram KH, Lopez-Davila MF, Munoz AJ, and Garvey WT. Limitations in the use of indices using glucose and insulin levels to predict insulin sensitivity: impact of race and gender and superiority of the indices derived from oral glucose tolerance test in African Americans. *Diabetes Care.* 2013;36(4):845-53.
36. Bergman RN, Finegood DT, and Kahn SE. The evolution of beta-cell dysfunction and insulin resistance in type 2 diabetes. *Eur J Clin Invest.* 2002;32 Suppl 3:35-45.
37. Fan W, Atkins AR, Yu RT, Downes M, and Evans RM. Road to exercise mimetics: targeting nuclear receptors in skeletal muscle. *J Mol Endocrinol.* 2013;51(3):T87-T100.

38. Lin J, Wu H, Tarr PT, Zhang CY, Wu Z, Boss O, et al. Transcriptional co-activator PGC-1 alpha drives the formation of slow-twitch muscle fibres. *Nature*. 2002;418(6899):797-801.
39. Mason RR, and Watt MJ. Unraveling the roles of PLIN5: linking cell biology to physiology. *Trends Endocrinol Metab*. 2015;26(3):144-52.
40. Hinkle RT, Hodge KM, Cody DB, Sheldon RJ, Kobilka BK, and Isfort RJ. Skeletal muscle hypertrophy and anti-atrophy effects of clenbuterol are mediated by the beta2-adrenergic receptor. *Muscle Nerve*. 2002;25(5):729-34.
41. Nolan CJ, Madiraju MS, Delghingaro-Augusto V, Peyot ML, and Prentki M. Fatty acid signaling in the beta-cell and insulin secretion. *Diabetes*. 2006;55 Suppl 2:S16-23.
42. Prentki M, Matschinsky FM, and Madiraju SR. Metabolic signaling in fuel-induced insulin secretion. *Cell Metab*. 2013;18(2):162-85.
43. Jezek P, Jaburek M, Holendova B, and Plecita-Hlavata L. Fatty Acid-Stimulated Insulin Secretion vs. Lipotoxicity. *Molecules*. 2018;23(6).
44. Distel RJ, Robinson GS, and Spiegelman BM. Fatty acid regulation of gene expression. Transcriptional and post-transcriptional mechanisms. *The Journal of biological chemistry*. 1992;267(9):5937-41.
45. Heine M, Fischer AW, Schlein C, Jung C, Straub LG, Gottschling K, et al. Lipolysis Triggers a Systemic Insulin Response Essential for Efficient Energy Replenishment of Activated Brown Adipose Tissue in Mice. *Cell Metab*. 2018.
46. Magkos F, Fraterrigo G, Yoshino J, Luecking C, Kirbach K, Kelly SC, et al. Effects of Moderate and Subsequent Progressive Weight Loss on Metabolic Function and Adipose Tissue Biology in Humans with Obesity. *Cell Metab*. 2016;23(4):591-601.
47. Sui W, Li H, Yang Y, Jing X, Xue F, Cheng J, et al. Bladder drug mirabegron exacerbates atherosclerosis through activation of brown fat-mediated lipolysis. *Proceedings of the National Academy of Sciences of the United States of America*. 2019;116(22):10937-42.
48. Hanssen MJ, Hoeks J, Brans B, van der Lans AA, Schaart G, van den Driessche JJ, et al. Short-term cold acclimation improves insulin sensitivity in patients with type 2 diabetes mellitus. *Nature medicine*. 2015;21(8):863-5.
49. van der Lans AA, Hoeks J, Brans B, Vijgen GH, Visser MG, Vosselman MJ, et al. Cold acclimation recruits human brown fat and increases nonshivering thermogenesis. *The Journal of clinical investigation*. 2013;123(8):3395-403.
50. Yoneshiro T, Aita S, Matsushita M, Kayahara T, Kameya T, Kawai Y, et al. Recruited brown adipose tissue as an antiobesity agent in humans. *The Journal of clinical investigation*. 2013;123(8):3404-8.
51. Hanssen MJ, van der Lans AA, Brans B, Hoeks J, Jardon KM, Schaart G, et al. Short-term Cold Acclimation Recruits Brown Adipose Tissue in Obese Humans. *Diabetes*. 2016;65(5):1179-89.
52. Vijgen GH, Bouvy ND, Teule GJ, Brans B, Schrauwen P, and van Marken Lichtenbelt WD. Brown adipose tissue in morbidly obese subjects. *PLoS one*. 2011;6(2):e17247.
53. Chondronikola M, Volpi E, Borsheim E, Porter C, Saraf MK, Annamalai P, et al. Brown Adipose Tissue Activation Is Linked to Distinct Systemic Effects on Lipid Metabolism in Humans. *Cell Metab*. 2016;23(6):1200-6.
54. Fischer AW, Shabalina IG, Mattsson CL, Abreu-Vieira G, Cannon B, Nedergaard J, et al. UCP1 inhibition in Cidea-overexpressing mice is physiologically counteracted by brown adipose tissue hyperrecruitment. *American journal of physiology Endocrinology and metabolism*. 2017;312(1):E72-E87.
55. Chouchani ET, Kazak L, Jedrychowski MP, Lu GZ, Erickson BK, Szpyt J, et al. Mitochondrial ROS regulate thermogenic energy expenditure and sulfenylation of UCP1. *Nature*. 2016;532(7597):112-6.

56. Fisher FM, and Maratos-Flier E. Understanding the Physiology of FGF21. *Annu Rev Physiol.* 2016;78:223-41.
57. Schwartz DR, and Lazar MA. Human resistin: found in translation from mouse to man. *Trends Endocrinol Metab.* 2011;22(7):259-65.
58. Chen BH, Song Y, Ding EL, Roberts CK, Manson JE, Rifai N, et al. Circulating levels of resistin and risk of type 2 diabetes in men and women: results from two prospective cohorts. *Diabetes Care.* 2009;32(2):329-34.
59. Heidemann C, Sun Q, van Dam RM, Meigs JB, Zhang C, Tworoger SS, et al. Total and high-molecular-weight adiponectin and resistin in relation to the risk for type 2 diabetes in women. *Ann Intern Med.* 2008;149(5):307-16.
60. Kern PA, Simsolo RB, and Fournier M. Effect of weight loss on muscle fiber type, fiber size, capillarity, and succinate dehydrogenase activity in humans. *The Journal of clinical endocrinology and metabolism.* 1999;84(11):4185-90.
61. Wilson JM, Loenneke JP, Jo E, Wilson GJ, Zourdos MC, and Kim JS. The effects of endurance, strength, and power training on muscle fiber type shifting. *J Strength Cond Res.* 2012;26(6):1724-9.
62. Ryall JG, and Lynch GS. The potential and the pitfalls of beta-adrenoceptor agonists for the management of skeletal muscle wasting. *Pharmacol Ther.* 2008;120(3):219-32.
63. Ohnuki Y, Umeki D, Cai W, Kawai N, Mototani Y, Shiozawa K, et al. Role of masseter muscle beta(2)-adrenergic signaling in regulation of muscle activity, myosin heavy chain transition, and hypertrophy. *J Pharmacol Sci.* 2013;123(1):36-46.
64. Lo JC, Ljubicic S, Leibiger B, Kern M, Leibiger IB, Moede T, et al. Adipsin is an adipokine that improves beta cell function in diabetes. *Cell.* 2014;158(1):41-53.
65. Stern JH, Rutkowski JM, and Scherer PE. Adiponectin, Leptin, and Fatty Acids in the Maintenance of Metabolic Homeostasis through Adipose Tissue Crosstalk. *Cell Metab.* 2016;23(5):770-84.
66. Holland WL, Miller RA, Wang ZV, Sun K, Barth BM, Bui HH, et al. Receptor-mediated activation of ceramidase activity initiates the pleiotropic actions of adiponectin. *Nature medicine.* 2011;17(1):55-63.
67. Sun K, Tordjman J, Clement K, and Scherer PE. Fibrosis and adipose tissue dysfunction. *Cell Metab.* 2013;18(4):470-7.
68. Kosteli A, Sugaru E, Haemmerle G, Martin JF, Lei J, Zechner R, et al. Weight loss and lipolysis promote a dynamic immune response in murine adipose tissue. *The Journal of clinical investigation.* 2010;120(10):3466-79.
69. Finlin BS, Zhu B, Confides AL, Westgate PM, Harfmann BD, Dupont-Versteegden EE, et al. Mast Cells Promote Seasonal White Adipose Beiging in Humans. *Diabetes.* 2017;66(5):1237-46.
70. Walton RG, Kosmac K, Mula J, Fry CS, Peck BD, Groshong JS, et al. Human skeletal muscle macrophages increase following cycle training and are associated with adaptations that may facilitate growth. *Sci Rep.* 2019;9(1):969.
71. Finlin BS, Zhu B, Boyechko T, Westgate PM, Chia CW, Egan JM, et al. Effect of Rifaximin Treatment on Endotoxemia and Insulin Sensitivity in Humans. *J Endocr Soc.* 2019;3(9):1641-51.
72. Chen KY, Cypess AM, Laughlin MR, Haft CR, Hu HH, Bredella MA, et al. Brown Adipose Reporting Criteria in Imaging Studies (BARCIST 1.0): Recommendations for Standardized FDG-PET/CT Experiments in Humans. *Cell Metab.* 2016;24(2):210-22.
73. Walton RG, Zhu B, Unal R, Spencer M, Sunkara M, Morris AJ, et al. Increasing adipocyte lipoprotein lipase improves glucose metabolism in high fat diet-induced obesity. *The Journal of biological chemistry.* 2015;290(18):11547-56.

74. Rasouli N, Yao-Borengasser A, Varma V, Spencer HJ, McGehee RE, Jr., Peterson CA, et al. Association of scavenger receptors in adipose tissue with insulin resistance in nondiabetic humans. *Arterioscler Thromb Vasc Biol.* 2009;29(9):1328-35.

## Figure Legends

### **Figure 1. Flow chart of the study design and analysis of the research**

**participants.** Sixty seven research subjects were assessed, and 39 were randomized into three drug treatment groups. The results for subjects in the pioglitazone and combination therapy groups will be presented in a future publication. Thirteen subjects were in the mirabegron treatment group, and all completed the study.

### **Figure 2. Mirabegron treatment improves glucose homeostasis in research participants who are obese and insulin-resistant.**

Subjects were treated with mirabegron (50 mg/day) for 12 weeks. Oral glucose tolerance tests (OGTT) and euglycemic clamps were performed at baseline and after treatment. A) OGTT results and area under the curve for all subjects are presented (n=12). Data represent mean  $\pm$  SEM and OGTT data were analyzed by 2-way repeated measures ANOVA; area under the curve data were analyzed by a paired, 2-tailed Student's t test. B) We performed euglycemic clamping at an insulin infusion rate of 1.0 mU/kg/min and determined the glucose infusion rate (GIR) before and after treatment. The data are represented as mean  $\pm$  SEM (n=13) and were analyzed by a paired, 2-tailed Student's t test. C) The insulinogenic index was determined from the results of the oral glucose tolerance test. The data are represented as mean  $\pm$  SEM (n=12) and were analyzed by a paired, 2-tailed Student's t test. D) The disposition index is the product of insulin sensitivity (panel C) and the insulinogenic index (panel D). The data are represented as mean  $\pm$  SEM (n=12) and were analyzed by a paired, 2-tailed Student's t test; \*P<0.05; \*\*P<0.01, \*\*\*P<0.001; \*\*\*\*P<0.0001. E) BAT volume was quantified by PET-CT scans before and after treatment. Eight subjects had no BAT at baseline, and BAT did not increase after treatment of these subjects. F) The change in SC WAT beiging was calculated as the difference in UCP1 protein expression before and after treatment. The change in the disposition index (panel 1D) and the change in UCP1 in SC WAT were analyzed by regression analysis. The Spearman correlation coefficient and P-value are indicated.

### **Figure 3. Mirabegron treatment reduces skeletal muscle triglyceride, but not**

**toxic lipids and promotes fiber type switching to type 1 fibers.** We extracted lipids from skeletal muscle, which was obtained from vastus lateralis biopsies and determined the level of the indicated lipid as described in methods. A) triglyceride, B) diglyceride, and C) ceramide levels before and after mirabegron treatment were determined. D through G) The mRNA expression of genes in muscle was determined by real-time RT-PCR. H) A representative image of muscle stained for MyHC I, MyHC IIa, and MyHCIIx before and after mirabegron treatment (scale bar: 50  $\mu$ m). I through L) Quantification of type I, type IIa, and type IIx fibers is shown; the data are expressed as percentage of total fibers. The data are represented as mean  $\pm$  SEM and were analyzed by a paired, 2-tailed Student's t test; \*P<0.05; \*\*P<0.01; (n=12 to 13).

### **Figure 4. Adipocyte conditioned medium isolated from adipocytes treated with mirabegron induces PGC1 $\alpha$ expression in human myotubes in vitro.**

We treated differentiated human adipocytes with or without 100 nM mirabegron for 16 hours and isolated the conditioned medium as described in Methods. We made an additional control by adding mirabegron to CM after the CM was isolated from the adipocytes. We

then incubated human myotubes with 0.025% DMSO (vehicle control), mirabegron (25 nM), adipocyte CM (25%), mirabegron treated adipocyte CM (25%), or adipocyte CM plus mirabegron (25%) as indicated. The final concentration of mirabegron was 25 nM. The data are represented as mean  $\pm$  SEM and were analyzed by one-way ANOVA and a Tukey multiple comparison test; \*P<0.05; \*\*\*P<0.001; (n=3).

**Figure 5. Mirabegron treatment stimulates lipolysis.** A) 0.5 g adipose tissue from the SC WAT biopsy was placed in medium and kept at 37°C for 1 hr. The level of glycerol was determined in the adipose tissue explant conditioned medium before and after treatment. B) Plasma NEFA levels were determined before and after treatment. The data are represented as mean  $\pm$  SEM and were analyzed by a paired, 2-tailed Student's t test; \*P<0.05; \*\*P<0.01; (n=13).

**Figure 6. Mirabegron treatment increases alternatively activated macrophages in SC WAT.** To characterize macrophage polarization, adipose tissue sections were doubly stained for (A) CD86/68 (M1) and (B) CD163/68 (M2). C) UCP1 is present in CD163 positive cells in SC WAT. Yellow arrows point to UCP1/CD163/DAPI positive cells (scale bar: 50 microns). D) UCP/CD163 positive cells were quantified in SC WAT before and after mirabegron treatment. The data are represented as mean  $\pm$  SEM and were analyzed by a paired, 2-tailed Student's t test; \*\*P<0.01; \*\*\*P<0.001; (n=13).

**Figure 7. Mirabegron treatment reduces State 4 respiration but does not increase uncoupled respiration in purified mitochondria isolated from SC WAT.** We purified mitochondria and analyzed the bioenergetics using an Oxytherm before and after mirabegron treatment as described in Methods. This involves the sequential addition of adenosine diphosphate (ADP), oligomycin (Oligo), free fatty acid (FFA; 60  $\mu$ M linoleic acid), fatty acid free BSA, and trifluoromethoxy carbonylcyanide phenylhydrazone (FCCP; 10  $\mu$ M). A and B) The oxygen consumption rates (OCRs) before and after treatment are shown. C) The difference between oligomycin and BSA was calculated before and after treatment. The data are represented as mean  $\pm$  SEM were analyzed by a Wilcoxon matched-pairs signed rank test; \*P=0.05; (n=12).

**Table 1. Baseline characteristics of study subjects and treatment responses.**

	Mirabegron <sup>a</sup>		P-value <sup>b</sup>
	Pre	Post	
<b>Number (Gender M/F)</b>	13 (2/11)		
<b>Age (years)</b>	54.8 ± 2.2		
<b>BMI (kg/m<sup>2</sup>)</b>	32.4 ± 1.1		
<b>Weight (kg)</b>	88.0 ± 2.6	87.5 ± 2.6	0.34
<b>Systolic BP (mmHg)</b>	127.8 ± 4.8	125.5 ± 3.5	0.42
<b>Diastolic BP (mmHg)</b>	79.8 ± 2.3	81.4 ± 2.6	0.61
<b>Heart Rate (beats / min)</b>	68.7 ± 1.6	70.7 ± 1.8	0.32
<b>Fasting Glucose (mg/dl)</b>	97.0 ± 2.8	95.8 ± 3.1	0.49
<b>Fasting Insulin (μU/mL)</b>	13.2 ± 2.7	14.4 ± 2.3	0.4
<b>120 min Glucose (mg/dl)</b>	135.3 ± 7.5	109.8 ± 6.4	<0.01
<b>HbA1c (%)</b>	5.6 ± 0.1	5.4 ± 0.1	0.01
<b>TG (mg/dl)</b>	144.0 ± 22.9	130.1 ± 18.0	0.35
<b>Cholesterol (mg/dl)</b>	215.7 ± 11.2	205.7 ± 11.6	0.09
<b>HDL (mg/dl)</b>	56.6 ± 5.1	55.9 ± 4.7	0.71
<b>LDL (mg/dl)</b>	132.9 ± 7.8	125.4 ± 8.6	0.15

<sup>a</sup>Research participants were treated with mirabegron (50 mg/day) for 12 weeks. Data represent mean ± SEM (n=13). <sup>b</sup>Data were analyzed by paired, two-tailed Student's t-tests.

**Table 2. Changes in SC WAT gene expression caused by mirabegron.**

<b>Gene symbol<sup>a</sup></b>	<b>Function</b>	<b>Fold Change</b>	<b>P-value</b>
Fabp4	Fatty acid metabolism	1.22	<0.01
RBP4	Secreted factor	1.24	<0.01
TIMP2	ECM	0.85	<0.01
COL6A1	ECM	0.89	0.02
angiopoietin 3	Angiogenesis	0.81	0.03
DGAT2	Lipid metabolism	1.24	0.03
angiopoietin 4	Angiogenesis	1.19	0.03
MMP-2	ECM	0.69	0.03
PPARG 2	Transcription factor	1.18	0.04
Resistin	Secreted factor	0.67	0.04
FGF21	Secreted factor	1.21	0.04
CerS6	Lipid metabolism	1.11	0.04
PKC alpha	Kinase	0.87	0.05
Elastin	ECM	0.76	0.05
GM-CSF	Cytokine	0.83	0.05
MMP14	ECM	0.88	0.05

<sup>a</sup>Research participants were treated with mirabegron (50 mg/day) for 12 weeks, and gene expression was measured at baseline and after treatment. Data represent mean  $\pm$  SEM (n=13). <sup>b</sup>Data were analyzed by paired, two-tailed Student's t-tests. Additional information is available in Table S5.

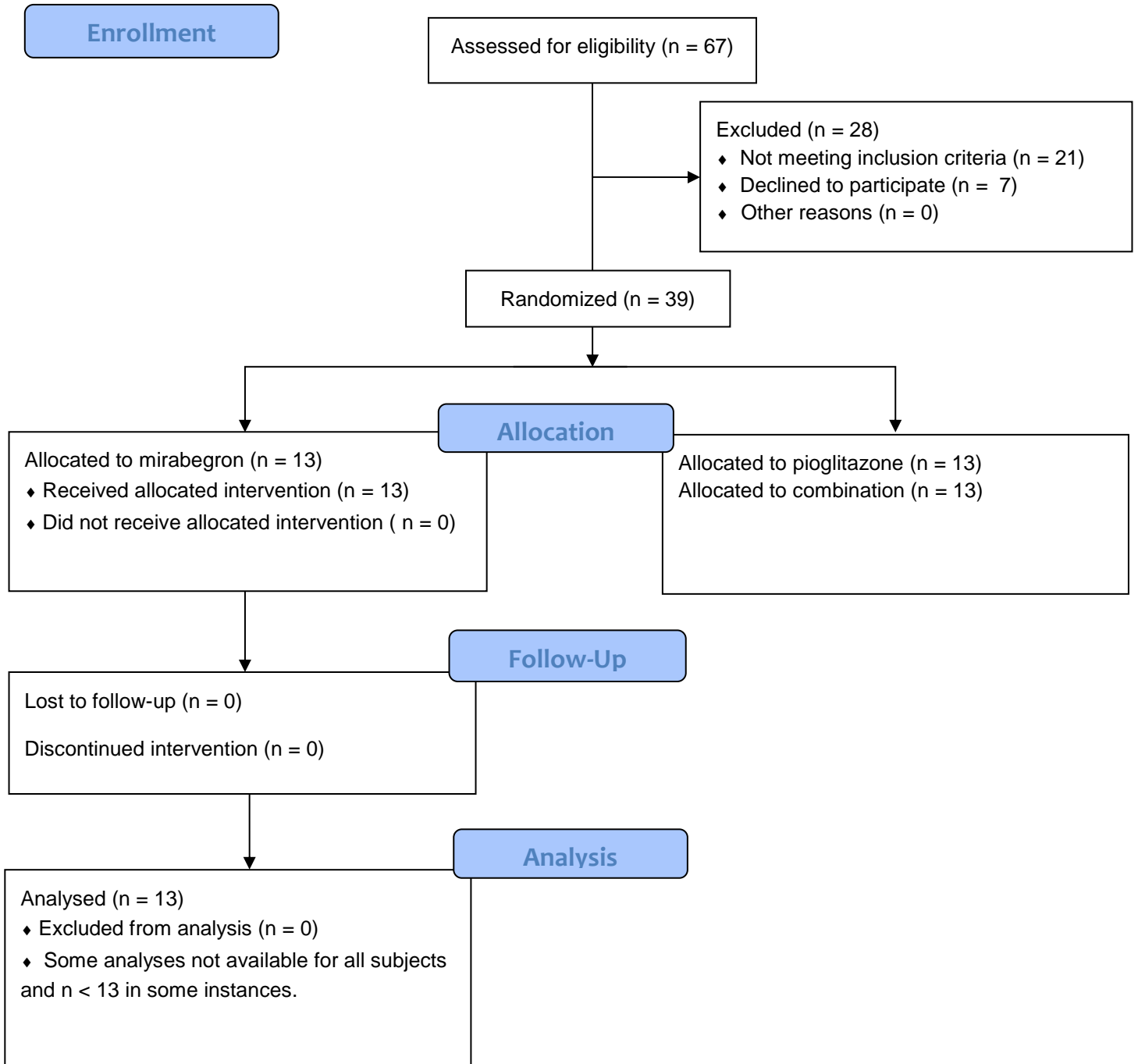


**Figure 1. Flow chart of the study design and analysis of the research participants.** Sixty seven research subjects were assessed, and 39 were randomized into three drug treatment groups. The results for subjects in the pioglitazone and combination therapy groups will be presented in a future publication. Thirteen subjects were in the mirabegron treatment group, and all completed the study.

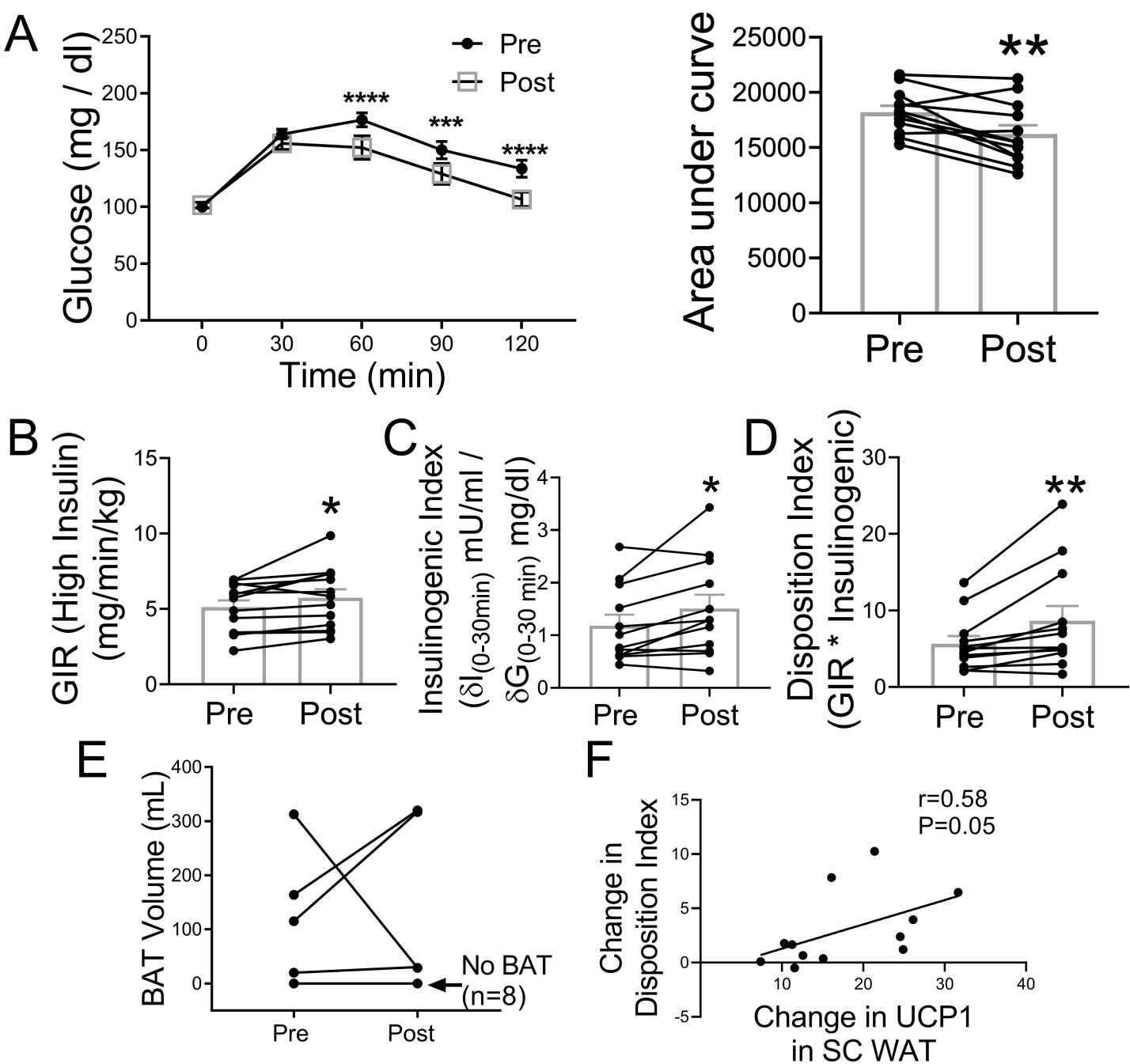


**Figure 2. Mirabegron treatment improves glucose homeostasis in research participants who are obese and insulin-resistant.** Subjects were treated with mirabegron (50 mg/day) for 12 weeks. Oral glucose tolerance tests (OGTT) and euglycemic clamps were performed at baseline and after treatment. A) OGTT results and area under the curve for all subjects are presented (n=12). Data represent mean  $\pm$  SEM and OGTT data were analyzed by 2-way repeated measures ANOVA; area under the curve data were analyzed by a paired, 2-tailed Student's t test. B) We performed euglycemic clamping at an insulin infusion rate of 1.0 mU/kg/min and determined the glucose infusion rate (GIR) before and after treatment. The data are represented as mean  $\pm$  SEM (n=13) and were analyzed by a paired, 2-tailed Student's t test. C) The insulinogenic index was determined from the results of the oral glucose tolerance test. The data are represented as mean  $\pm$  SEM (n=12) and were analyzed by a paired, 2-tailed Student's t test. D) The disposition index is the product of insulin sensitivity (panel C) and the insulinogenic index (panel D). The data are represented as mean  $\pm$  SEM (n=12) and were analyzed by a paired, 2-tailed Student's t test; \* $P < 0.05$ ; \*\* $P < 0.01$ ; \*\*\* $P < 0.001$ ; \*\*\*\* $P < 0.0001$ . E) BAT volume was quantified by PET-CT scans before and after treatment. Eight subjects had no BAT at baseline, and BAT did not increase after treatment of these subjects. F) The change in SC WAT being was calculated as the difference in UCP1 protein expression before and after treatment. The change in the disposition index (panel 1D) and the change in UCP1 in SC WAT were analyzed by regression analysis. The Spearman correlation coefficient and P-value are indicated.

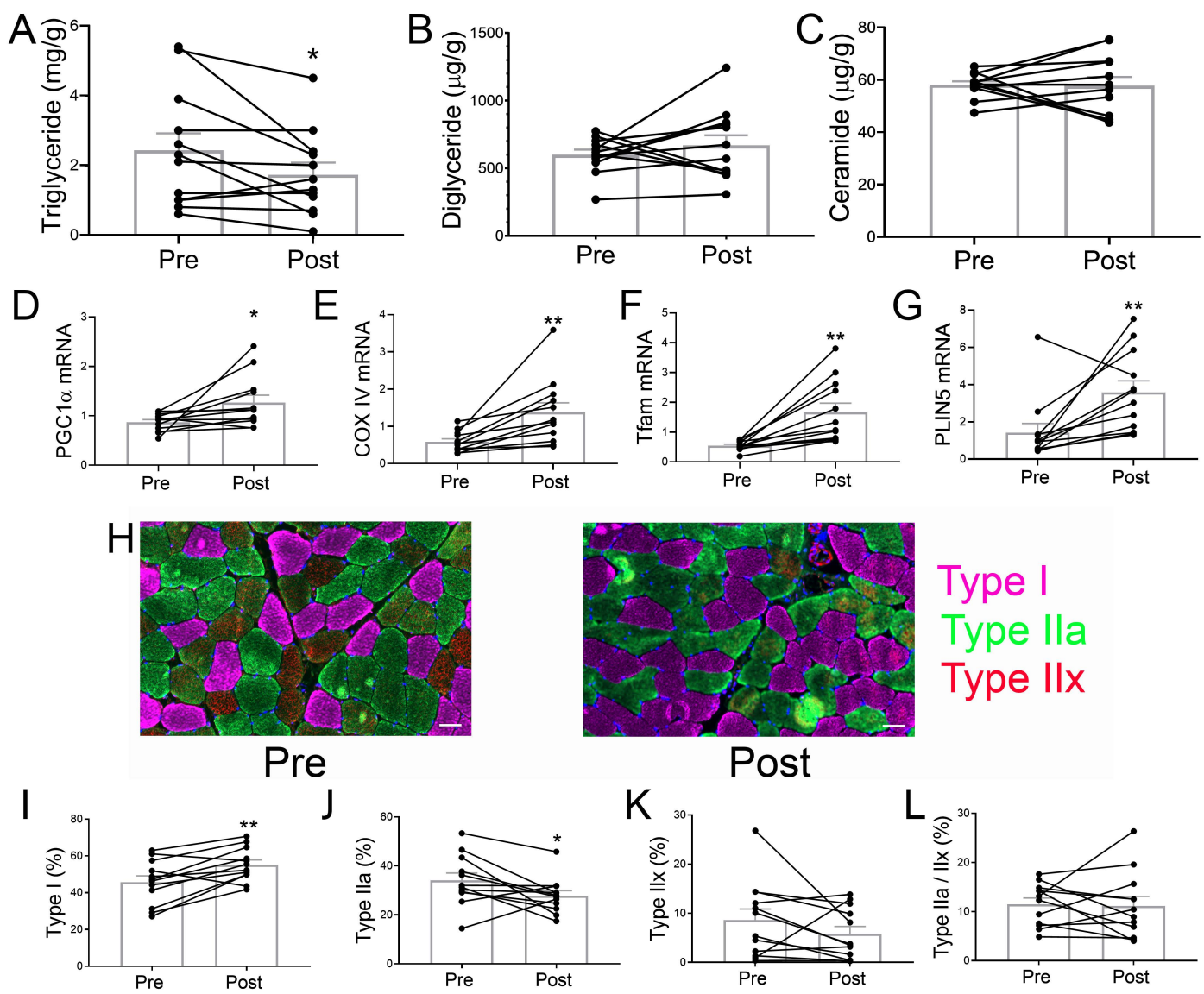


**Figure 3. Mirabegron treatment reduces skeletal muscle triglyceride, but not toxic lipids and promotes fiber type switching to type 1 fibers.** We extracted lipids from skeletal muscle, which was obtained from vastus lateralis biopsies and determined the level of the indicated lipid as described in methods. A) triglyceride, B) diglyceride, and C) ceramide levels before and after mirabegron treatment were determined. D through G) The mRNA expression of genes in muscle was determined by real-time RT-PCR. H) A representative image of muscle stained for MyHC I, MyHC IIa, and MyHCIIx before and after mirabegron treatment (scale bar: 50  $\mu\text{m}$ ). I through L) Quantification of Type I, type IIa, and type IIx fibers is shown; the data are expressed as percentage of total fibers. The data are represented as mean  $\pm$  SEM and were analyzed by a paired, 2-tailed Student's t test; \* $P < 0.05$ ; \*\* $P < 0.01$ ; (n=12 to 13).

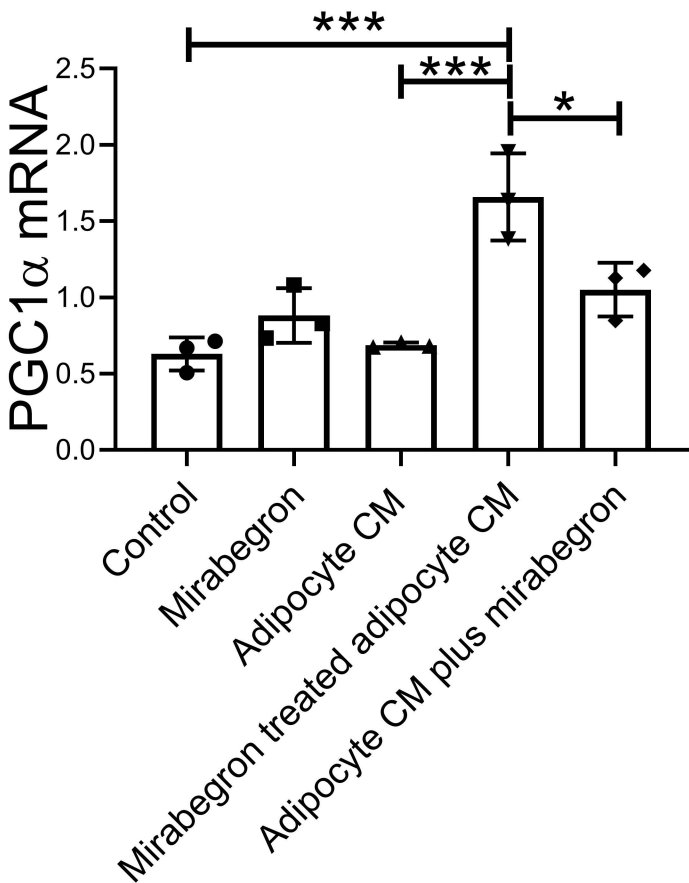


**Figure 4. Adipocyte conditioned medium isolated from adipocytes treated with mirabegron induces PGC1 $\alpha$  expression in human myotubes in vitro.** We treated differentiated human adipocytes with or without 100 nM mirabegron for 16 hours and isolated the conditioned medium as described in Methods. We made an additional control by adding mirabegron to CM after the CM was isolated from the adipocytes. We then incubated human myotubes with 0.025% DMSO (vehicle control), mirabegron (25 nM), adipocyte CM (25%), mirabegron treated adipocyte CM (25%), or adipocyte CM plus mirabegron (25%) as indicated. The final concentration of mirabegron was 25 nM. The data are represented as mean  $\pm$  SEM and were analyzed by one-way ANOVA and a Tukey multiple comparison test; \* $P < 0.05$ ; \*\*\* $P < 0.001$ ; (n=3).

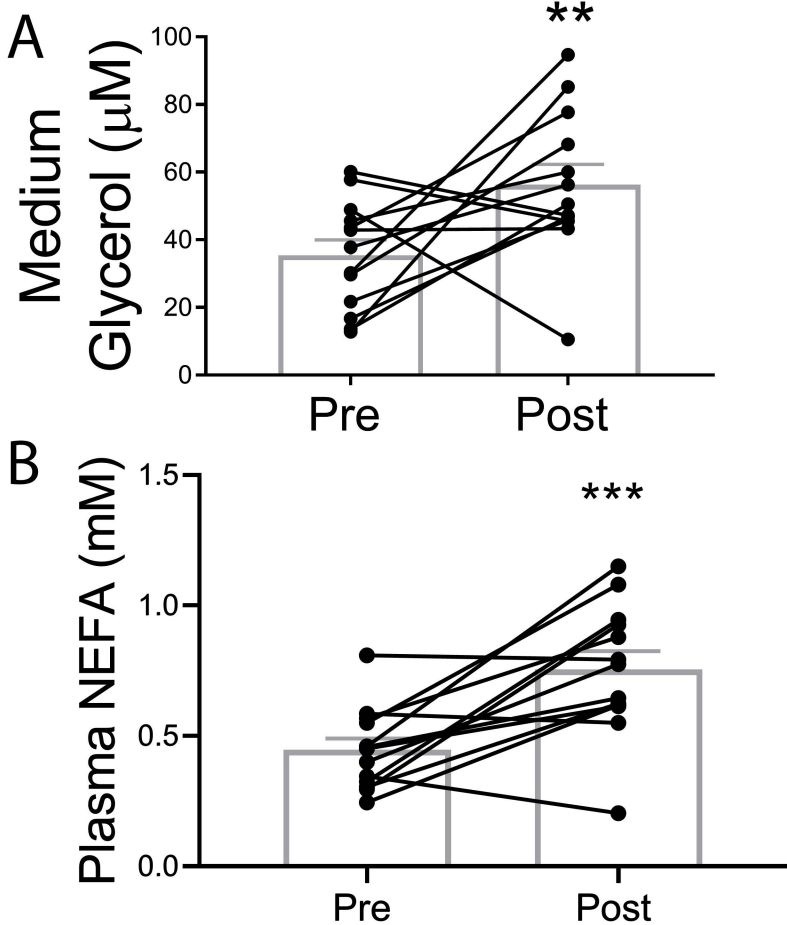


**Figure 5. Mirabegron treatment stimulates lipolysis.** A) 0.5 g adipose tissue from the SC WAT biopsy was placed in medium and kept at 37°C for 1 hr. The level of glycerol was determined in the adipose tissue explant conditioned medium before and after treatment. B) Plasma NEFA levels were determined before and after treatment. The data are represented as mean  $\pm$  SEM and were analyzed by a paired, 2-tailed Student's t test; \* $P < 0.05$ ; \*\* $P < 0.01$ ; ( $n = 13$ ).

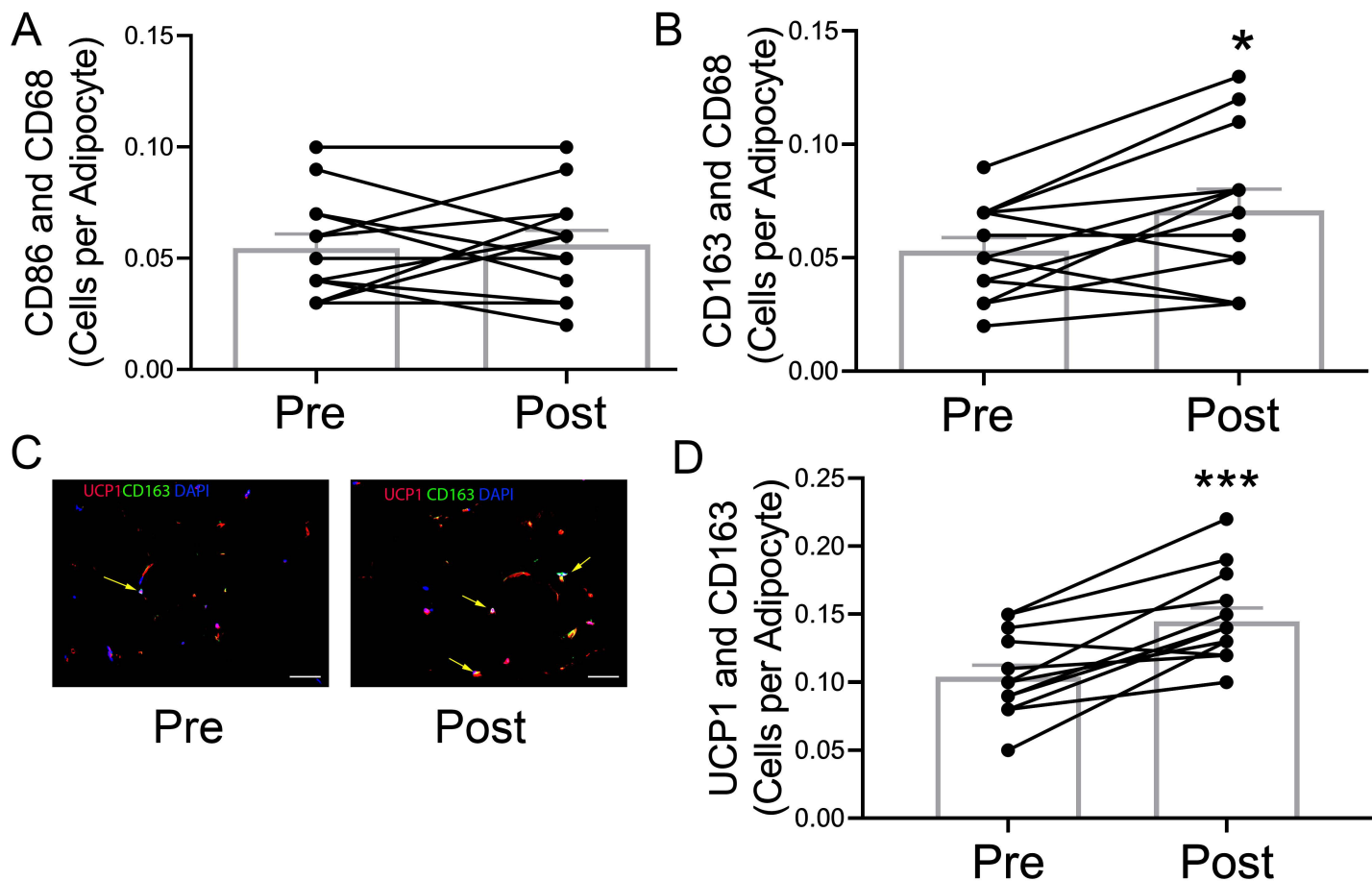


**Figure 6. Mirabegron treatment increases alternatively activated macrophages in SC WAT.** To characterize macrophage polarization, adipose tissue sections were doubly stained for (A) CD86/68 (M1) and (B) CD163/68 (M2). C) UCP1 is present in CD163 positive cells in SC WAT. Yellow arrows point to UCP1/CD163/DAPI positive cells (scale bar: 50 microns). D) UCP/CD163 positive cells were quantified in SC WAT before and after mirabegron treatment. The data are represented as mean  $\pm$  SEM and were analyzed by a paired, 2-tailed Student's *t* test; \*\* $P < 0.01$ ; \*\*\* $P < 0.001$ ; ( $n = 13$ ).

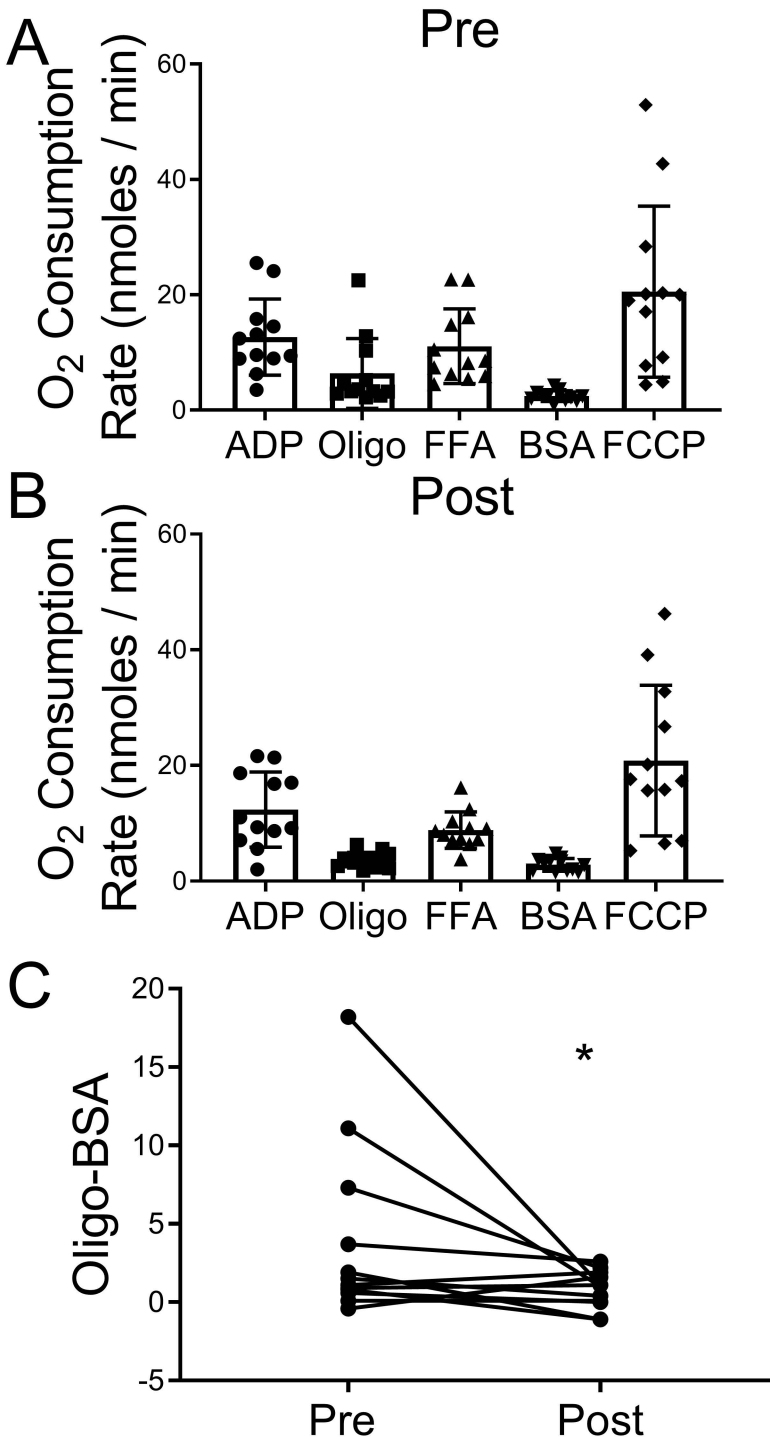


**Figure 7. Mirabegron treatment reduces State 4 respiration but does not increase uncoupled respiration in purified mitochondria isolated from SC WAT.** We purified mitochondria and analyzed the bioenergetics using an Oxytherm before and after mirabegron treatment as described in Methods. This involves the sequential addition of adenosine diphosphate (ADP), oligomycin (Oligo), free fatty acid (FFA; 60  $\mu$ M linoleic acid), fatty acid free BSA, and trifluoromethoxy carbonyl cyanide phenylhydrazine (FCCP; 10  $\mu$ M). A and B) The oxygen consumption rates (OCRs) before and after treatment are shown. C) The difference between oligomycin and BSA was calculated before and after treatment. The data are represented as mean  $\pm$  SEM were analyzed by a Wilcoxon matched-pairs signed rank test; \*P=0.05; (n=12).